



ELSEVIER

Contents lists available at [SciVerse ScienceDirect](http://www.sciencedirect.com)

Radiation Physics and Chemistry

journal homepage: www.elsevier.com/locate/radphyschem

Radiation synthesis and characterization of nanosilver/gelatin/carboxymethyl chitosan hydrogel

Ying Zhou^{a,b}, Yinghui Zhao^{a,b}, Lu Wang^a, Ling Xu^{a,b,*}, Maolin Zhai^c, Shicheng Wei^{b,d,**}

^a College of Engineering, Peking University, Beijing 100871, China

^b Center for Biomedical Materials and Tissue Engineering, Academy for Advanced Interdisciplinary Studies, Peking University, Beijing 100871, China

^c Beijing National Laboratory for Molecular Sciences, Department of Applied Chemistry, College of Chemistry and Molecular Engineering, Peking University, Beijing 100871, China

^d Department of Oral and Maxillofacial Surgery, School and Hospital of Stomatology, Peking University, Beijing 100081, China

ARTICLE INFO

Article history:

Received 14 November 2011

Accepted 9 January 2012

Available online 20 January 2012

Keywords:

Nanosilver

Radiation

Gelatin

Carboxymethyl Chitosan

Hydrogel

Wound dressing

ABSTRACT

A series of antibacterial hydrogels were fabricated from an aqueous solution of AgNO₃, gelatin and carboxymethyl chitosan (CM-chitosan) by radiation-induced reduction and crosslinking at ambient temperature. The nanosilver particles were in situ synthesized accompanying with the formation of gelatin/CM-chitosan hydrogel. Transmission Electron Microscope and UV–vis analysis have verified the formation and homogeneous distribution of nanosilver particles in the hydrogel matrix. The nanosilver/gelatin/CM-chitosan hydrogels possessed interconnected porous structure, had a compressive modulus of 44 to 56 kPa, and could absorb 62 to 108 times of deionized water to its dry weight. Furthermore, the hydrogels were found to have sound antibacterial effect on *Escherichia coli* (*E. coli*), and their antibacterial ability could be significantly enhanced by the increasing of AgNO₃ content. The comprehensive results of this study suggest that nanosilver/gelatin/CM-chitosan hydrogels have potential as an antibacterial wound dressing.

© 2012 Elsevier Ltd. All rights reserved.

1. Introduction

Infection and large amount of tissue fluid loss remain the leading causes of morbidity in burn wound management and other supportive care regimens. Therefore, an ideal wound dressing should have high water-absorption ability, excellent biocompatibility and anti-inflammation effects (Kumar et al., 2010).

Silver and silver ions have been known as effective antimicrobial agents for a long time. Nanosilver particles have extremely large surface area to contact with bacteria or fungi. They could bind to microbial DNA and the sulphhydryl groups of the metabolic enzymes in bacterial electron transport chain. The former will prevent the replication of bacteria, and the latter will inactivate them (Maki and Tambyah, 2001; Thomas et al., 2007). Hence, owing to their excellent antimicrobial activity, nanosilver particles have been applied to a wide range of healthcare products such as burn dressings, scaffolds, skin donors and medical devices (Hillyer and Albrecht, 2001; Jain and Pradeep, 2005).

Due to the lack of sufficient chemical and physical stability, the application of nanosilver particles on wound care products has been restricted to some extent (Murthy et al., 2008). Therefore, nanosilver particle should be attached to the carriers, such as polymer matrix, prior to several applications (Ho et al., 2004; Mohan et al., 2007). However, most of the preparation procedures of hybrid systems were started with a prefabricated nanometal, followed by the addition of nanometal particle into polymer component. For instance, a nanoparticle-loaded gels was typically prepared by swelling a gel in the dispersion of nanometal particles; mixing a colloidal solution of nanometal particles with an aqueous polymer solution, followed by solvent evaporation (El-Sherif et al., 2011). In each case, the agglomeration of nanosilver particles, and the burst release of large amount of nanosilver to the body fluid and blood system, would occur and caused regional toxicity (Klasen, 2000; Tsipouras et al., 1997). Therefore, the research efforts are heading towards the synthesis of nanosilver particles contained polymeric network with certain antimicrobial activity and low cytotoxicity.

Gelatin, is a hydrolysis derivative of collagen, and contains a number of biological functional groups like amino acids (Marois et al., 1995). Compared with collagen, gelatin has less antigenicity and more stable physicochemical properties. CM-chitosan, a water-soluble derivative of chitosan, has been used in a wide variety of applications in biomedical field owing to its good biocompatibility and biodegradability. In our previous work,

* Corresponding author at: College of Engineering, Peking University, Beijing 100871, China. Tel.: +86 10 62769915.

** Corresponding author at: Department of Oral and Maxillofacial Surgery, School and Hospital of Stomatology, Peking University, Beijing 100081, China. Tel.: /fax: +86 10 62753404.

E-mail addresses: lingxu@pku.edu.cn (L. Xu), sc-wei@pku.edu.cn (S. Wei).

a series of gelatin/CM-chitosan hydrogels were fabricated by radiation-induced crosslinking at ambient temperature. The hydrogels possessed high water absorption capacity, similar compressive modulus with soft tissue, controllable biodegradation and excellent biocompatibility (Yang et al., 2010). Further addition of nanosilver particles to gelatin/CM-chitosan hydrogel is expected to improve the antimicrobial activity of the hydrogel and reduce the risk of inflammation during wound healing procedure.

Ling Huang et al. proposed an ultraviolet light irradiation method to synthesize gold or silver nanoparticles in CM-chitosan solution, and found that CM-chitosan served as both reducing agent for cations and stabilizing agent for nanoparticles (Huang et al., 2008; Huang et al., 2007). Manmohan Kumar et al. prepared Ag clusters by reduction of Ag^+ in polyvinyl alcohol (PVA) hydrogel using γ -irradiation (Kumar et al., 2005). Therefore, it can be expected that nanosilver particle will be in situ synthesized during the formation of gelatin/CM-chitosan hydrogel by ionization radiation.

In this study, nanosilver/gelatin/CM-chitosan hydrogels were prepared by radiation crosslinking and reduction simultaneously, resulting in a stable and homogeneous distribution of nanosilver particles in the matrix. Effects of AgNO_3 concentrations on the distribution and morphology of nanosilver particles in hydrogel matrix were studied. Physical properties of the hydrogels such as the porous structure, swelling behavior and compressive strength were investigated. Besides, the antibacterial performance of the hydrogels against Gram-negative *Escherichia coli* (*E. coli*) was tested qualitatively and quantitatively. The nanosilver/gelatin/CM-chitosan hydrogel is expected to be a novel wound healing material with combined advantages of gelatin/CM-chitosan hydrogel and anti-inflammation ability of nanosilver particles.

2. Materials and methods

2.1. Materials

Gelatin (product G1890, 300 g Bloom, porcine skin, Type A) was purchased from Sigma Chemical Co. Ltd. CM-chitosan powder (degree of deacetylation 96.5%; Mw 70, 000) was purchased from Qingdao Honghai Co. Ltd, China. Silver nitrate (AgNO_3) and other reagents were of analytical grade.

2.2. Preparation of nanosilver/gelatin/CM-chitosan hydrogels

The nanosilver/gelatin/CM-chitosan composite hydrogels were typically prepared as follows. First, different concentrations of AgNO_3 solution (0–10 mM) were prepared by dissolve AgNO_3 powders in deionized water. Next, gelatin and CM-chitosan powders with a weight ratio of 2:3 and total concentration of 10 wt% were mixed homogeneously in AgNO_3 solution at 50 °C. After that, the mixture was mixed by an ARE-310 hybrid mixer (Japan Thinky Co. Ltd.) for 20 min to form a homogenous polymer solution. Finally, the solution was filled into test tubes (inner diameter 10 mm) and subjected for γ -irradiation with 30 kGy at ambient temperature using a ^{60}Co facility. The optimal preparation conditions, such as the composition of gelatin/CM-chitosan and absorbed dose, were determined in our previous work to obtain hydrogels with desired properties (Yang et al., 2010).

2.3. Characterization of nanosilver particles in the gelatin/CM-chitosan hydrogels

2.3.1. Transmission electron microscope

The morphology of nanosilver particles in the prepared composite hydrogels was observed under a Tecnai F30 transmission

electron microscopy (TEM) operated at 300 kV. For TEM measurements, the samples were prepared by dropping 10–20 μl of the dehydrated alcohol dispersion containing finely grinded lyophilized nanosilver/gelatin/CM-chitosan composite hydrogels on the grid of copper mesh and dried at room temperature. The average diameter and size distribution were calculated from 50 pieces of nanosilver particles in the TEM image (Tankhiwale and Bajpai, 2010).

2.3.2. UV-vis analysis

The UV-vis spectra of nanosilvers in the nanosilver/gelatin/CM-chitosan composite hydrogels were recorded by a Hitachi Model 3010 spectrophotometer. The scan was performed in the range of 200 to 700 nm with an interval of 0.5 nm. The hydrogels were cut into cylinders ($\Phi 10 \times 5$ mm) and completely degraded in 10 ml of 1 mg ml^{-1} collagenase enzyme solutions before subjected to UV-vis analysis.

2.4. Characterization of the nanosilver/gelatin/CM-chitosan hydrogels

2.4.1. Scanning electron microscope

The morphology of the hydrogels was observed with Scanning Electron Microscope (SEM) (HITACHI S-4800, Japan) at an accelerating voltage of 1 kV. Equilibrium swollen hydrogel samples were lyophilized before observation.

2.4.2. Swelling behavior in deionized water

The hydrogels were cut into cylinders with diameter of 10 mm and thickness of 5 mm, and then the samples were immersed in beakers containing 150 ml deionized water at 37 °C for 24 h to get a maximal degree of swelling. After that, the samples were withdrawn from the solution and the surface solution was gently removed by filter paper. The degree of swelling was calculated using Eq. (1). Six parallel samples were measured to achieve an average value.

$$\text{Degree of Swelling} = \frac{m_2}{m_1 \times 0.1} \quad (1)$$

where m_1 , m_2 and 0.1 represent weight of the sample before and after swelling, and the polymer concentration in the hydrogels, respectively.

2.4.3. Gel fraction

Cylindrical hydrogel ($\Phi 10 \times 5$ mm) samples were immersed in deionized water for 24 h at 37 °C to remove the sol part. After that, the samples were dried at 60 °C in vacuum. The gel fraction was calculated using Eq. (2):

$$\text{Gel Fraction} = \frac{m_4}{m_3 \times 0.1} \times 100\% \quad (2)$$

where m_3 , m_4 and 0.1 represent initial weight of the sample, dried sample and the polymer concentration in the hydrogels, respectively. Six parallel samples were measured to get an average.

2.4.4. Mechanical properties

The compressive strength of the samples was tested by universal material testing instrument (Instron 5843). Hydrogels cylinders with the size of $\Phi 10 \times 10$ mm were prepared. The compressive test was conducted with a constant strain rate of 1 mm min^{-1} until 90% reduction in specimen height. The compressive strength was calculated from the stress-strain curve. Compressive modulus was calculated as the slope of the initial linear portion of the curve. The samples were measured in triplicate to get an average.

2.5. Antibacterial performance of the nanosilver/gelatin/CM-chitosan hydrogels

2.5.1. Bacterial incubation

E. coli (ATCC 25,922), which is Gram-negative and widespread intestinal parasite of mammals, was cultivated at 37 °C in sterilized LB broth (peptone 10 g, yeast extract 5 g, NaCl 10 g, distilled water 1000 mL) at 150 rpm in a rotary shaker for 16 h. Then the bacterial suspension was diluted by LB broth into certain concentration.

2.5.2. Bacterial testing of inhibition halo

Antibacterial performance of the hydrogels with different concentration of nanosilver was evaluated by modified Kirby Bauer technique (Yu et al., 2007). Briefly, 50 μ l bacteria medium (with a concentration of ca. 10^6 colony forming units (CFU)/ml of *E. coli*) was dispensed onto an agar plate, then the hydrogel disks ($\Phi 10 \times 5$ mm) were placed on the agar plate and incubated for 12 h at 37 °C. After that, the bacterial growth inhibition halos around the samples were observed and their diameters were measured.

2.5.3. Bacterial testing of inhibition kinetics curve

To examine the kinetics of bacterial growth or inhibition ratio of nanosilver/gelatin/CM-chitosan hydrogels, 0.4 g of gelatin/CM-chitosan and nanosilver/gelatin/CM-chitosan hydrogels were immersed in 40 ml of germ-containing nutrient solution with a bacterial concentration of approximately 10^5 CFU/ml. The incubation was performed at 37 °C and oscillated at a frequency of 150 rpm for 24 hours. Pure bacteria medium (10^5 CFU/ml) was also incubated and served as control. The bacterial broth medium was taken out at regular intervals, and the optical density (OD) of the medium at 600 nm was measured by a UV-vis spectrophotometer. The inhibition ratios of the nanosilver/gelatin/CM-chitosan hydrogels were calculated by Eq. (3):

$$\text{Inhibition Ratio(\%)} = 100 - 100 \times \frac{A_t - A_0}{A_{\text{con}} - A_0} \quad (3)$$

where A_0 was the OD of bacterial broth medium before incubation; A_t and A_{con} were the ODs of hydrogel and control sample after incubation for desired time, respectively.

3. Result and discussion

3.1. In situ synthesis of nanosilver particles in gelatin/CM-chitosan Hydrogel

3.1.1. TEM analysis

A reasonable nanosilver particle release amount should be considered to achieve sufficient antibacterial ability and biosafety.

Literature results indicated that the scaffold with 50 mM AgNO_3 was non-toxic to rat osteoprogenitor cells and human osteosarcoma cell lines (Selvamurugan et al., 2011). Therefore, the concentration of AgNO_3 solutions to prepare the hydrogel was chosen to be in the range of 0 to 10 mM. With the increasing of AgNO_3 concentrations, radiolytic reduction of Ag^+ in gelatin/CM-chitosan solutions yielded hydrogels colored from yellow to dark brown (Fig. 1(a)). The immobilization of the silver nanoparticles throughout the hydrogel networks could be ascribed to the slow diffusion of the Ag^+ within the networks. The formed silver nanoparticles exhibited excellent stability over a few months inside the hydrogel networks.

HADF images and EDX analysis of nanosilver/gelatin/CM-chitosan composite hydrogels with AgNO_3 concentrations of 5 mM are depicted in Fig. 1 (b) and (c). It is apparent that the nanoparticles showed a uniformly spherical shape and were well dispersed within the gelatin/CM-chitosan crosslinked network. The existence of elemental silver in the hydrogel, as detected by EDX, confirmed the formation of nanosilver particles in the gelatin/CM-chitosan network.

The radiation crosslinking mechanism of gelatin and CM-chitosan has been discussed in our previous work (Yang et al., 2010). Under irradiation, the network between gelatin and CM-chitosan was formed, resulting in the excellent water adsorption ability of gelatin/CM-chitosan hydrogels. Herein, water molecules are ionized and excited by γ ray to yield several kinds of free radicals such as e^- , H_2O^+ and H_2O^* , etc. These radicals can recombine with each other and form reductive radicals (for example, hydrated electrons), which could strongly induce the reduction of Ag^+ (Ershov et al., 1993). The amino ($-\text{NH}_2$) and hydroxyl ($-\text{OH}$) groups of chitosan and gelatin act as templates to bind with Ag^+ , thus leading to the uniform distribution of nanosilver particles in the gelatin/CM-chitosan matrix (Bajpai et al., 2011).

TEM was used for visual observation of the nanosilver particles with typical morphology as shown in fig 2, which represents the images and size distributions of the nanosilver particles in gelatin/CM-chitosan composite hydrogels with AgNO_3 concentrations of 2, 5 and 10 mM, respectively. Spherical nanosilver particles were found to disperse homogeneously in all samples with slight aggregates. In addition, hydrogels prepared with higher concentration of Ag^+ had larger nanosilver particles (Chen et al., 2000). The histogram of 2 mM hydrogel represented that the large majority of particles were in the range of 3–6 nm in diameter. However, the size increased to the range of 5–10 nm at the 5 mM samples. As the concentration increased to 10 mM, the size of nanosilver particles was found to be in the range of 10–30 nm, with certain amount of aggregations. During the radiation, when the concentration of AgNO_3 was low, Ag^+ was

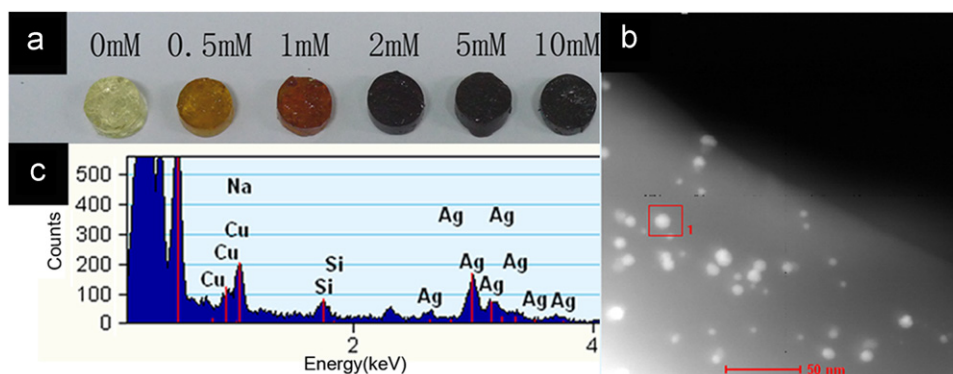


Fig. 1. (a) Images of hydrogels with AgNO_3 concentrations of 0 to 10 mM. (b) HADF image and (c) EDX analysis of nanosilver/gelatin/CM-chitosan composite hydrogel with AgNO_3 concentration of 5 mM.

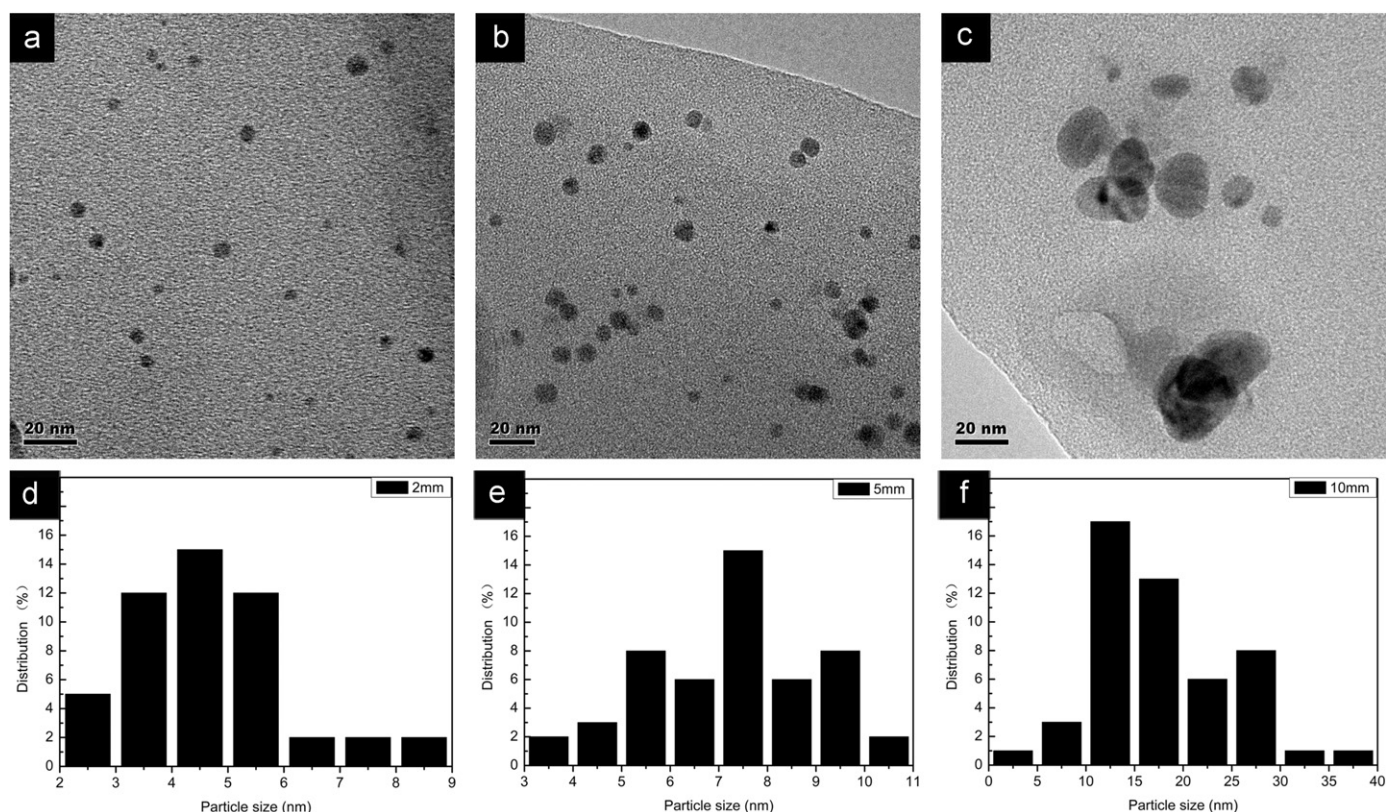


Fig. 2. TEM images of the nanosilver particles of nanosilver/gelatin/CM-chitosan composite hydrogels with AgNO₃ concentrations of (a) 2 mM, (b) 5 mM, and (c) 10 mM. Size distributions of the nanosilver particles of nanosilver/gelatin/CM-chitosan composite hydrogels with AgNO₃ concentrations of (d) 2 mM, (e) 5 mM, and (f) 10 mM.

far from each other. Highly dense gelatin/CM-chitosan networks tend to establish more intra-inter molecular attractions between gel networks resulting in less free space in the hydrogel networks (Mohan et al., 2007). Therefore, the surrounding Ag⁺ particles were prevented from aggregating. The dense gelatin/CM-chitosan networks would help to stabilize and regulate the size of nanosilver particles. However, when the amount of Ag⁺ increased, the newly formed nanosilver particles were likely to aggregate with previously formed ones, leading to the increase of nanoparticle size.

3.1.2. UV–vis analysis

To prove the formation of nanosilver particles in the networks, we carried out UV–vis absorption studies. Characteristic peak of nanosilver particles at around 410 nm in UV–vis spectrum can be ascribed to the surface plasmon resonance (SPR) effect of quantum size (Fig. 3). Nanosilver particles (ca. 2.5 nm) embedded in silica colloids have shown the absorption bands in the same region (Wang and Asher, 2001). Comparison of six samples in the UV–vis spectra indicated that increasing the AgNO₃ concentration during the preparation of hydrogel raised the intensity of the absorbance peak and induced a slightly red shift. The SPR plays a major role in the determination of optical absorption spectra of nanometal particles, which shifts to a higher wavelength with the increase in particle size (Jing et al., 2007). As discussed in previous sections, with the increase of AgNO₃ concentration, the size of nanoparticles increased, resulting in the red shift of the peak. On the other hand, plasmon absorption increment in the UV–vis spectra represents the formation of a higher number of nanosilver particles. Further, the result clearly confirms that no aggregation or cluster formation of silver particles because of complete absence of peaks at 335 and 560 nm (Mohan et al., 2010).

3.2. Characterization of nanosilver/gelatin/CM-chitosan Hydrogel

3.2.1. SEM analysis

It is well known that a porous structure is important for the transport of oxygen and promotion of drainage during wound healing, and a three-dimensional network structure is crucial to absorbing and keeping large amount of water in hydrogel materials (Yu et al., 2007).

In this study, as shown in Fig. 4, porous three-dimensional network structures with smooth surface morphology were formed in all hydrogels. The prepared nanosilver particles were not visible in the SEM images because the size was rather small. For the hydrogel samples, the pore diameter distributions were between 200 and 600 μm, which were expected to be sufficient for the permeation of nutrients, oxygen and waste products from the cells.

3.2.2. Swelling behavior

An ideal wound dressing should be able to absorb wound exudate and provide a wet environment for the wound so that sufficient swelling ability is crucial for hydrogel wound dressing. Swelling behavior of the nanosilver/gelatin/CM-chitosan hydrogels is shown in Fig. 5. All the hydrogels show a swelling ratio higher than 60, which is sufficient for the application as hydrogel wound dressing. The maximal degree of swelling was raised significantly by increasing the concentrations of AgNO₃ solutions, but decreased slightly when the concentration reached 10 mM. It is well known that the swelling of hydrogel is induced by the electrostatic repulsion of the ionic charges of its network, which blocks the aggregation of the polymer chains and acts to expand the hydrogel (Yiamsawas et al., 2007). Besides, the nanosilver particles of different size inside the hydrogel have different

surface charges, which caused the different swelling ability of the hydrogels (Mohan et al., 2006; Murthy et al., 2008). Furthermore, the increased maximal degree of swelling implied that nanosilver particles would reduce the crosslinking density.

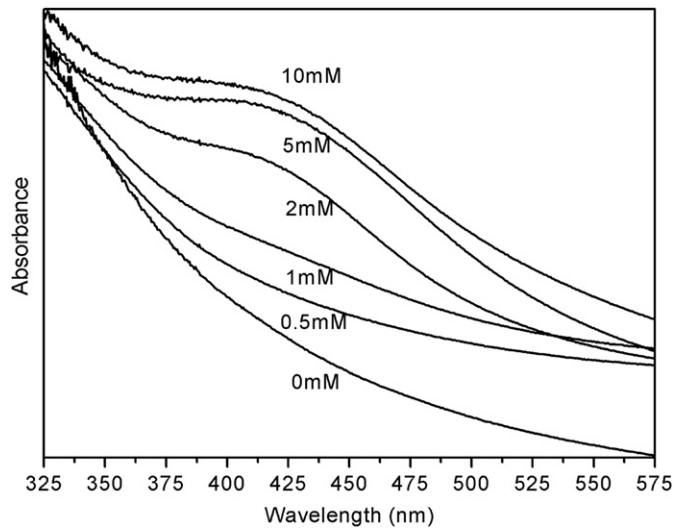


Fig. 3. UV-vis spectra of nanosilver particles in the hydrogels.

To evaluate the degree of crosslinking quantitatively, gel fraction of the hydrogels was investigated. Under γ -irradiation, CM-chitosan crosslinked and degraded concurrently, and radiation crosslinking was dominant in the condition of this study

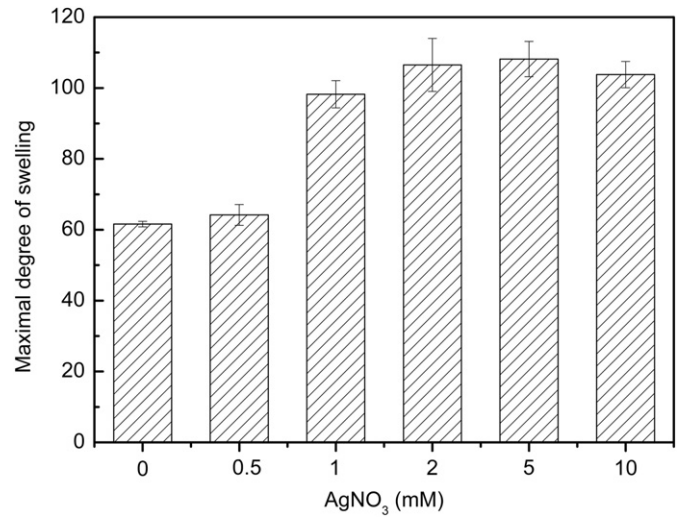


Fig. 5. Maximal degree of swelling of nanosilver/gelatin/CM-chitosan hydrogels in deionized water with AgNO₃ concentrations of 0, 0.5, 1, 2, 5 and 10 mM.

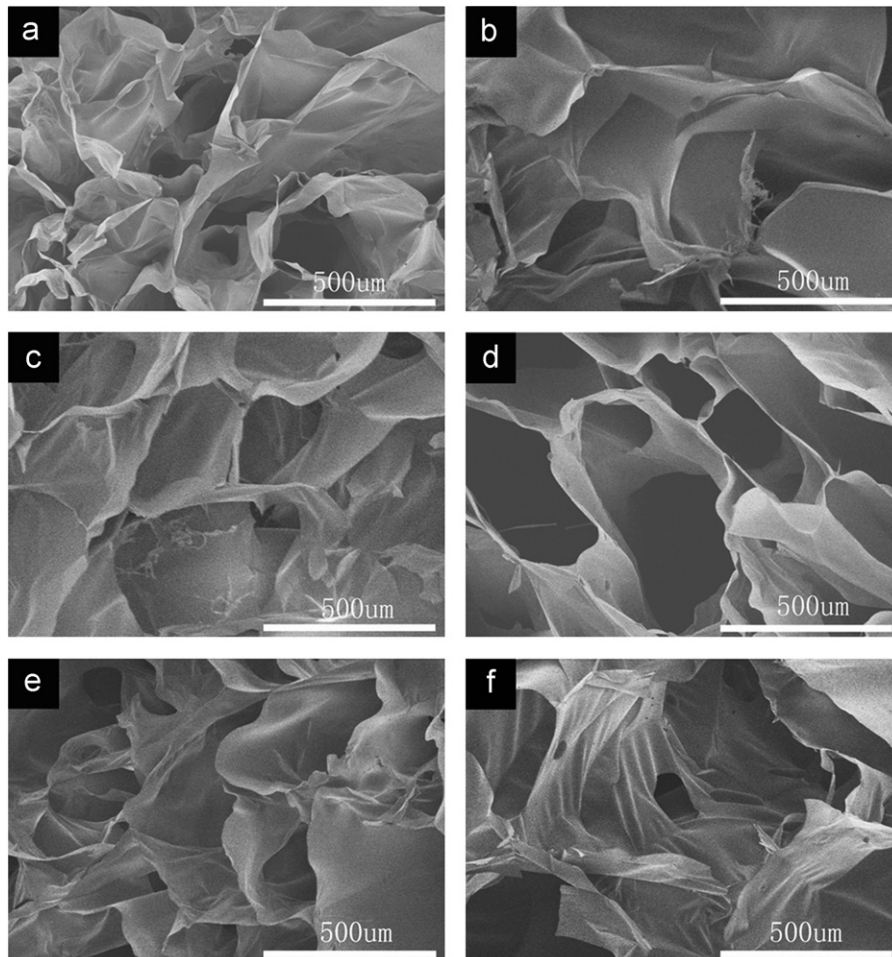


Fig. 4. SEM images of nanosilver/gelatin/CM-chitosan composite hydrogels with AgNO₃ concentrations of (a) 0 mM, (b) 0.5 mM, (c) 1 mM, (d) 2 mM, (e) 5 mM, and (f) 10 mM.

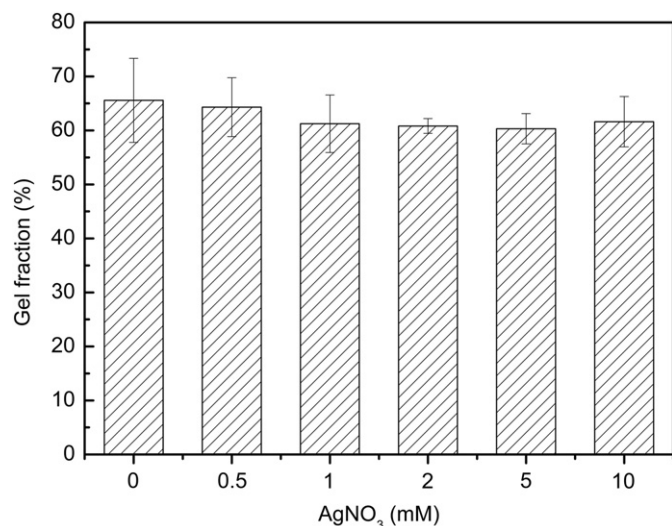


Fig. 6. Gel fractions of nanosilver/gelatin/CM-chitosan hydrogels with AgNO₃ concentrations of 0, 0.5, 1, 2, 5 and 10 mM.

Table 1
Mechanical properties of hydrogels as a function of AgNO₃ concentrations.

AgNO ₃ Concentration (mM)	Hydrogels	
	Compressive modulus (kPa)	Compressive strength (kPa)
0	55.7 ± 2.7	209.2 ± 52.1
0.5	54.2 ± 2.8	195.6 ± 23.8
1	54.3 ± 3.9	202.6 ± 28.8
2	51.6 ± 9.2	176.1 ± 17.5
5	43.9 ± 2.8	167.6 ± 32.7
10	46.6 ± 4.5	315.1 ± 40.5

(Yang et al., 2010). Therefore, although a physically stable composite hydrogel could be formed, certain portion of the composite hydrogel was sol. The gel fraction of nanosilver/gelatin/CM-chitosan composite hydrogels versus AgNO₃ concentrations is shown in Fig. 6. The gel fractions of all samples were between 61 and 66%, and decreased slightly with the addition of AgNO₃. Lower gel fraction corresponded to less crosslinking, and resulted in the expansion of hydrogel. Nanosilver particles would interact with –OH and –NH₂ groups in the gelatin/CM-chitosan matrix via hydrogen bonding (Karthikeyan, 2005; Khanna et al., 2005; Krkljes et al., 2007). As a result, nanosilver particles would interfere the radiation crosslinking, and lead to the slightly decrease of gel fraction. However, the samples with 10 mM AgNO₃ content present a slightly increase. This might be attributed to the agglomeration of nanosilver particles, which limited the amount of particles in the gel-particle interface.

3.2.3. Mechanical properties

The hydrogel was prepared to a mechanical stable form, which will be easy to be handled and will benefit for further clinical application. The compressive modulus and compressive strength of the hydrogels were measured, as shown in Table 1. For nanosilver-composite hydrogels prepared with 0–10 mM AgNO₃, the mechanical properties of hydrogels slightly reduced with the increase of nanosilver particles. These results corresponded to the performance of gel fraction, which was analyzed in the previous section. Reduced gel fraction indicated a network with lower

crosslinking degree, thus resulted in the decrease in mechanical strength. Moreover, the presence of nanosilver in hydrogels would cause a dispersed interruption of nanosilver particles on the gelatin/CM-chitosan matrix and also lead to the slightly decrease in the mechanical properties (Nguyen et al., 2011). However, all the nanosilver/gelatin/CM-chitosan hydrogel samples had proper mechanical strength to support the soft tissue regeneration (Lu et al., 2009).

3.3. In vitro antibacterial effect

3.3.1. Bacterial testing of inhibition halo

Antibacterial ability of the nanosilver contained hydrogels and blank gelatin/CM-chitosan hydrogel were preliminarily evaluated by a modified Kirby Bauer technique (Melaiye et al., 2005). After 12 h incubation at 37 °C, the nanosilver/gelatin/CM-chitosan hydrogels clearly showed antibacterial ability against Gram-negative *E. coli*. As showed in Fig. 7(a), the zones of inhibition were 13.5, 17.8, and 19.6 mm when the nanosilver concentrations were 2, 5 and 10 mM, respectively. As a control, no significant inhibition halo was found in the gelatin/CM-chitosan hydrogel. These results showed that the antibacterial activity increased with the increase of nanosilver concentration. Therefore, it can be concluded that the antibacterial activity was mainly ascribed to the presence of nanosilver in hydrogels, and crosslinked gelatin/CM-chitosan hydrogel served as a stable carrier for nanosilver particles.

3.3.2. Bacterial testing of inhibition kinetics curve

As shown in Fig. 7(b), the antibiotic ability against *E. coli*, expressed as inhibition ratio, was enhanced with the increase of nanosilver content in the hydrogels. The hydrogel with 10 mM nanosilver content inhibited more than 99% of the *E. coli* by adding 0.4 g sample to 40 ml bacterial suspension (10⁵ CFU/ml). The antibacterial activity was found to be sustained, as inhibition ratio kept above 97% even after 12 h of incubation. When the nanosilver content decreased to 5 mM, the maximum inhibition ratio was around 50%. However, when the nanosilver content further decreased to 2 mM, the ratio decreased to 26%. The gelatin/CM-chitosan hydrogel merely showed a weak inhibition effect to *E. coli*, which was ascribed to certain antibacterial ability of CM-chitosan (Chen et al., 2002).

For all the samples, the antibacterial activity presented maximum and then decreased, which was also reported in the literatures (Pal et al., 2007; Sondi and Salopek-Sondi, 2004). When the hydrogels were immersed into the suspension, large amount of nanosilver particles were released and contributed to the initial inhibition of bacterial growth. In the meantime, these particles interacted with intracellular substances of the destroyed cells and formed coagulations, which resulted in the decrease of nanosilver concentration in the aqueous circumstance (Sondi and Salopek-Sondi, 2004). With gradually reduced release amount of nanosilver, the consumption of nanosilver dominated. Therefore, resumed growth of bacteria occurred when the concentration of nanosilver decreased below the minimum inhibitory concentration (Grasso et al., 1978).

In all, besides their effective and sustained antibacterial ability, as discussed in this section, nanosilver/gelatin/CM-chitosan composite hydrogels performed homogeneous distribution of nanosilver particles. Meanwhile, they possessed biomimetic composition, excellent swelling ability, interconnected porous structures and proper mechanical properties, which favored their application as wound dressing.

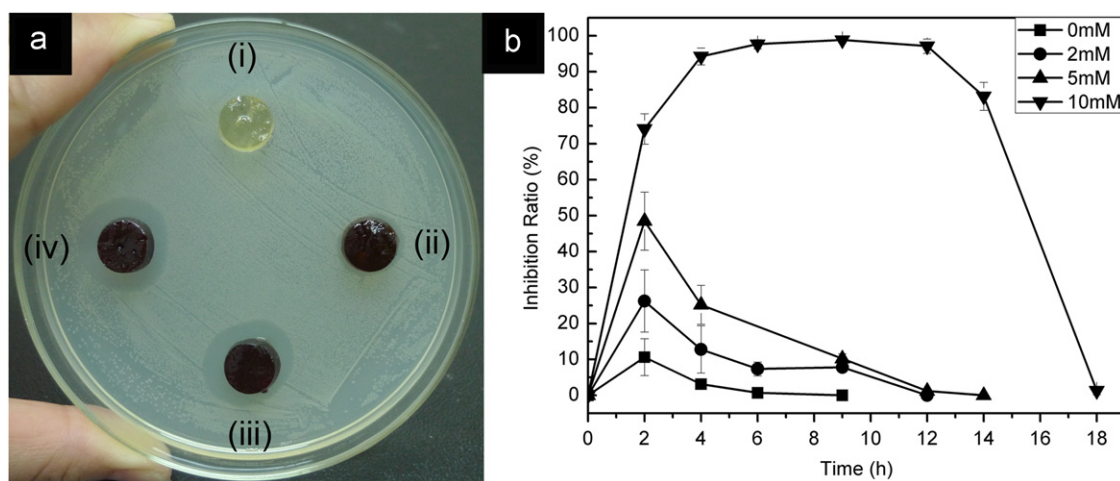


Fig. 7. (a) Antibacterial activity of hydrogels against *E. coli*. The specimens used were hydrogels with AgNO_3 concentrations of (i) 0 mM, (ii) 2 mM, (iii) 5 mM, and (iv) 10 mM. (b) Inhibition ratio kinetics curves of hydrogels against *E. coli*. The specimens used were hydrogels with AgNO_3 concentrations of 0, 2, 5 and 10 mM.

4. Conclusion

Nanosilver/gelatin/CM-chitosan composite hydrogels were synthesized by a green and simple fabrication method, i.e. radiation-induced reduction and crosslinking. The nanosilver particles showed homogeneous distribution inside the hydrogels, and the size of particles increased with increasing concentration of AgNO_3 . The synthesized hydrogels possessed highly interconnected porous network structure, excellent and adjustable water retention capacity, and proper compressive strength, which would meet the basic criteria for wound covering material. In addition, the present of nanosilver imparted antibacterial ability to the hydrogels via controlled release of nanosilver particles and degradation of the hydrogel. Sound antibacterial ability against *E. coli* could be reached with the presence of 10 mM nanosilver within hydrogel. Therefore, the nanosilver/gelatin/CM-chitosan hydrogels have the potential to be antibacterial wound covering materials.

Acknowledgment

This work was supported by the National Natural Science Foundation of China (no. 21103004), National Key Technology R and D Program (2011BAB02B05), State Key Development Program for Basic Research of China (Grant 2007CB936103), Peking University Interdisciplinary and Emerging Disciplines Research Foundation (Grant PKUJC2009001). We thank Mr. Jiuqiang Li for his kind help in γ -irradiation.

References

- Bajpai, S.K., Thomas, V., Bajpai, M., 2011. In Situ Formation of Silver Nanoparticles within Chitosan-attached Cotton Fabric for Antibacterial Property. *J. Ind. Text* 40, 229–245.
- Chen, W.M., Yuan, Y., Yan, L.F., 2000. Preparation of organic/inorganic nanocomposites with polyacrylamide (PAM) hydrogel by Co-60 gamma irradiation. *Mater. Res. Bull.* 35, 807–812.
- Chen, X.G., Wang, Z., Liu, W.S., Park, H.J., 2002. The effect of carboxymethyl-chitosan on proliferation and collagen secretion of normal and keloid skin fibroblasts. *Biomaterials* 23, 4609–4614.
- El-Sherif, H., El-Masry, M., Kansoh, A., 2011. Hydrogels as Template Nanoreactors for Silver Nanoparticles Formation and Their Antimicrobial Activities. *Macromol. Res* 19, 1157–1165.
- Erskov, B.G., Janata, E., Henglein, A., Fojtik, A., 1993. Silver Atoms and Clusters in Aqueous-Solution-Absorption-Spectra and the Particle Growth in the Absence of Stabilizing Ag^+ Ions. *J. Phys. Chem* 97, 4589–4594.

- Grasso, S., Meinardi, G., Decarneri, I., Tamassia, V., 1978. New Invitro Model to Study Effect of Antibiotic Concentration and Rate of Elimination on Antibacterial Activity. *Antimicrob. Agents Chemother* 13, 570–576.
- Hillyer, J.F., Albrecht, R.M., 2001. Gastrointestinal persorption and tissue distribution of differently sized colloidal gold nanoparticles. *J. Pharm. Sci.* 90, 1927–1936.
- Ho, C.H., Tobis, J., Sprich, C., Thomann, R., Tiller, J.C., 2004. Nanoseparated polymeric networks with multiple antimicrobial properties. *Adv. Mater.* 16, 957–961.
- Huang, L., Zhai, M.L., Long, D.W., Peng, J., Xu, L., Wu, G.Z., Li, J.Q., Wei, G.S., 2008. UV-induced synthesis, characterization and formation mechanism of silver nanoparticles in alkaline carboxymethylated chitosan solution. *J. Nanopart. Res.* 10, 1193–1202.
- Huang, L., Zhai, M.L., Peng, J., Xu, L., Li, J.Q., Wei, G.S., 2007. Synthesis, size control and fluorescence studies of gold nanoparticles in carboxymethylated chitosan aqueous solutions. *J. Colloid Interface Sci.* 316, 398–404.
- Jain, P., Pradeep, T., 2005. Potential of silver nanoparticle-coated polyurethane foam as an antibacterial water filter. *Biotechnol. Bioeng* 90, 59–63.
- Jing, X.B., Yu, H.J., Xu, X.Y., Chen, X.S., Lu, T.C., Zhang, P.B., 2007. Preparation and antibacterial effects of PVA-PVP hydrogels containing silver nanoparticles. *J. Appl. Polym. Sci.* 103, 125–133.
- Karthikeyan, B., 2005. Spectroscopic studies on Ag-polyvinyl alcohol nanocomposite films. *PhyB* 364, 328–332.
- Khanna, P.K., Singh, N., Charan, S., Subbarao, V.V.V.S., Gokhale, R., Mulik, U.P., 2005. Synthesis and characterization of Ag/PVA nanocomposite by chemical reduction method. *Mater. Chem. Phys.* 93, 117–121.
- Klasen, H.J., 2000. A historical review of the use of silver in the treatment of burns. II. Renewed interest for silver. *Burns* 26, 131–138.
- Krkiljes, A.N., Marinovic-Cincovic, M.T., Kacarevic-Popovic, Z.M., Nedeljkovic, J.M., 2007. Radiolytic synthesis and characterization of Ag-PVA nanocomposites. *Eur. Polym. J.* 43, 2171–2176.
- Kumar, M., Varshney, L., Francis, S., 2005. Radiolytic formation of Ag clusters in aqueous polyvinyl alcohol solution and hydrogel matrix. *Radiat. Phys. Chem.* 73, 21–27.
- Kumar, P.T.S., Abhilash, S., Manzoor, K., Nair, S.V., Tamura, H., Jayakumar, R., 2010. Preparation and characterization of novel beta-chitin/nanosilver composite scaffolds for wound dressing applications. *Carbohydr. Polym.* 80, 761–767.
- Lu, M.H., Yu, W.N., Huang, Q.H., Huang, Y.P., Zheng, Y.P., 2009. A Hand-Held Indentation System for the Assessment of Mechanical Properties of Soft Tissues In Vivo. *ITIM* 58, 3079–3085.
- Maki, D.G., Tambyah, P.A., 2001. Engineering out the risk for infection with urinary catheters. *Emerging Infect. Dis* 7, 342–347.
- Marois, Y., Chakfe, N., Deng, X.Y., Marois, M., How, T., King, M.W., Guidoin, R., 1995. Carbodiimide Cross-Linked Gelatin—New Coating for Porous Polyester Arterial Prostheses. *Biomaterials* 16, 1131–1139.
- Melaiye, A., Sun, Z.H., Hindi, K., Milsted, A., Ely, D., Reneker, D.H., Tessier, C.A., Youngs, W.J., 2005. Silver(I)-imidazole cyclophane gem-diol complexes encapsulated by electrospun tectophilic nanofibers: Formation of nanosilver particles and antimicrobial activity. *J. Am. Chem. Soc.* 127, 2285–2291.
- Mohan, Y.M., Lee, K., Premkumar, T., Geckeler, K.E., 2007. Hydrogel networks as nanoreactors: A novel approach to silver nanoparticles for antibacterial applications. *Polymer* 48, 158–164.
- Mohan, Y.M., Premkumar, T., Lee, K., Geckeler, K.E., 2006. Fabrication of silver nanoparticles in hydrogel networks. *Macromol. Rapid Commun.* 27, 1346–1354.
- Mohan, Y.M., Vimala, K., Thomas, V., Varaprasad, K., Sreedhar, B., Bajpai, S.K., Raju, K.M., 2010. Controlling of silver nanoparticles structure by hydrogel networks. *J. Colloid Interface Sci.* 342, 73–82.

- Murthy, P.S.K., Mohan, Y.M., Varaprasad, K., Sreedhar, B., Raju, K.M., 2008. First successful design of semi-IPN hydrogel-silver nanocomposites: A facile approach for antibacterial application. *J. Colloid Interface Sci.* 318, 217–224.
- Nguyen, T.H., Kim, Y.H., Song, H.Y., Lee, B.T., 2011. Nano Ag loaded PVA nanofibrous mats for skin applications. *J. Biomed. Mater. Res. B Appl. Biomater* 96B, 225–233.
- Pal, S., Tak, Y.K., Song, J.M., 2007. Does the Antibacterial Activity of Silver Nanoparticles Depend on the Shape of the Nanoparticle? A Study of the Gram-Negative Bacterium *Escherichia coli*. *Appl. Environ. Microbiol* 73, 1712–1720.
- Selvamurugan, N., Saravanan, S., Nethala, S., Pattnaik, S., Tripathi, A., Moorthi, A., 2011. Preparation, characterization and antimicrobial activity of a bio-composite scaffold containing chitosan/nano-hydroxyapatite/nano-silver for bone tissue engineering. *Int. J. Biol. Macromol.* 49, 188–193.
- Sondi, I., Salopek-Sondi, B., 2004. Silver nanoparticles as antimicrobial agent: A case study on E-coli as a model for Gram-negative bacteria. *J. Colloid Interface Sci* 275, 177–182.
- Tankhiwale, R., Bajpai, S.K., 2010. Silver-Nanoparticle-Loaded Chitosan Lactate Films with Fair Antibacterial Properties. *J. Appl. Polym. Sci.* 115, 1894–1900.
- Thomas, V., Yallapu, M.M., Sreedhar, B., Bajpai, S.K., 2007. A versatile strategy to fabricate hydrogel-silver nanocomposites and investigation of their antimicrobial activity. *J. Colloid Interface Sci.* 315, 389–395.
- Tsipouras, N., Rix, C.J., Brady, P.H., 1997. Passage of silver ions through membrane-mimetic materials, and its relevance to treatment of burn wounds with silver sulfadiazine cream. *Clin. Chem* 43, 290–301.
- Wang, W., Asher, S.A., 2001. Photochemical incorporation of silver quantum dots in monodisperse silica colloids for photonic crystal applications. *J. Am. Chem. Soc.* 123, 12528–12535.
- Yang, C., Xu, L., Zhou, Y., Zhang, X.M., Huang, X., Wang, M., Han, Y., Zhai, M.L., Wei, S.C., Li, J.Q., 2010. A green fabrication approach of gelatin/CM-chitosan hybrid hydrogel for wound healing. *Carbohydr. Polym* 82, 1297–1305.
- Yiamsawas, D., Kangwansupamonkon, W., Chailapakul, O., Kiatkamjornwong, S., 2007. Synthesis and swelling properties of poly[acrylamide-co-(crotonic acid)] superabsorbents. *React. Funct. Polym.* 67, 865–882.
- Yu, H.J., Xu, X.Y., Chen, X.S., Lu, T.C., Zhang, P.B., Jing, X.B., 2007. Preparation and antibacterial effects of PVA-PVP hydrogels containing silver nanoparticles. *J. Appl. Polym. Sci.* 103, 125–133.